

Near-UV and optical spectroscopic investigation of late-type stars from the MIRA/*Oliver Observing Station*

Subhajeet KARMAKAR^{1,*}, Avrajit BANDYOPADHYAY², William Bruce WEAVER¹,
Riddhi SHEDGE^{1,3}, Jeewan Chandra PANDEY⁴, Daniel Vincent COTTON^{1,5}
and Jean PERKINS¹

¹ Monterey Institute for Research in Astronomy (MIRA), 200 Eighth Street, Marina, California 93933, USA

² University of Florida, Gainesville, Florida, 32611, USA

³ Monta Vista High School, 21840 McClellan Rd, Cupertino, California 95014, USA

⁴ Aryabhatta Research Institute of Observational Sciences (ARIES), Manora Peak, Nainital 263002, India

⁵ Western Sydney University, Locked Bag 1797, Penrith-South DC, NSW 1797, Australia

* Corresponding author: subhajeet09@gmail.com, sk@mira.org

This work is distributed under the Creative Commons CC-BY 4.0 Licence.

Paper presented at the 3rd BINA Workshop on “Scientific Potential of the Indo-Belgian Cooperation”, held at the Graphic Era Hill University, Bhimtal (India), 22nd–24th March 2023.

Abstract

Late-type stars are the most abundant in the galactic stellar population. These stars, with the similar internal structure to the Sun, are expected to have solar-like atmospheres. Investigating the stellar parameters and chemical abundances on late-type stars is essential to provide valuable constraints about stellar age, chemical evolution, and atmosphere of exoplanets. In this work, we present the study of the Near-UV and optical spectroscopic observation of three late-type stars: HR 8038, AC Her, HD 76446, as obtained from the 36-inch MIRA/*Oliver Observing Station*. We derived surface temperature, gravity, metallicity, and the chemical abundances of light element carbon in the stellar atmosphere. The elemental abundance of the carbon for HR 8038, AC Her, and HD 76446 are derived to be 95%, 97%, and 108%, respectively, of the solar value.

Keywords: stars: low-mass, star: abundances, stellar atmosphere, star: individual (HR 8038, AC Her, HD 76446)

1. Introduction

Most of the stellar population of our Galaxy consists of late-type stars (Bochanski et al., 2010). With partially- or fully-convective envelopes, late-type stars are expected to have solar-like atmospheres and magnetic activities (Priest, 2000; Karmakar, 2019). However, the stars present a wide range of temperature, gravity, metallicity, and elemental abundances that have

Table 1: Observation details of the Program stars.

Object	SpT	RA (hh:mm:ss.ss)	Dec (dd:mm:ss.ss)	Obs-Date	Exp Time (s)	V (mag)
HR 8038	F1	21:00:03.99	+07:30:58.28	2017-10-23	720	5.99
AC Her	F4	18:30:16.24	+21:52:00.60	2010-06-15	420	7.01
HD 76446	G2	08:56:33.11	+12:25:54.78	2010-02-17	1800	8.42

been found to vary significantly over time (Jofré et al., 2014; Bandyopadhyay et al., 2022; Karmakar et al., 2016, 2017, 2019, 2022, 2023). Therefore, a robust observational and theoretical investigation is essential. Investigating the elemental abundances of late-type stars provides key information for characterizing the stellar population of our Galaxy. carbon being the fourth most abundant element in the universe (after hydrogen, helium, and oxygen), is of particular interest in many fields of astrophysics, including stellar age determination (Bond et al., 2013; Romano et al., 2020; Zhang et al., 2021; Beverage et al., 2023), chemical evolution of galaxies (Chiappini et al., 2003; Carigi et al., 2005; Cescutti et al., 2009; Botelho et al., 2020; Gustafsson, 2022), and structure of exoplanets (Bond et al., 2010; Madhusudhan et al., 2012; Pelletier et al., 2021; Grant et al., 2023).

For the past two decades, the Monterey Institute for Research in Astronomy (MIRA) has observed hundreds of spectra of low-mass stars. In this paper, utilizing a subsample of this survey, we present an investigation of surface temperature, gravity, metallicity, and carbon abundances using the NUV and optical low-resolution spectra of three late-type stars: HR 8038, AC Her, and HD 76446. These F and G-type stars are located at a distance of 56.4 ± 1.6 , 1231 ± 44 , and 81.5 ± 0.9 pc, respectively (Bailer-Jones et al., 2018). Some basic information of these stars are shown in Table 1. We structured the paper as follows: Section 2 describes the observations and data analysis. Section 3 describes the models and methods utilized for atmospheric modeling and presents the results. Finally, in Section 4, we discuss the result and outlined the conclusions drawn from our study.

2. Observations and Data Analysis

The low-resolution ($\sim 5,000$) spectroscopic observations of three late-type stars have been carried out using the 36-inch F/10 classical Cassegrain Telescope mounted at the *Bernard M. Oliver Observing Station* (OOS; Weaver, 1975) of the *Monterey Institute for Research in Astronomy* (MIRA). The OOS is located at an elevation of 5010 feet on Chews Ridge in California – one of the best-seeing sites in the Pacific region ($\approx 1''1$; Hutter et al., 1997; Walker, 1970). For all three observations, the dual-port spectrograph (DPS; see Torres-Dodgen and Weaver, 1993) has been used with a 1200 lines per mm grating along with a back-illuminated 1024×255 ANDOR Camera (Model: DU420-BU; see Walker et al., 2007). The observations were performed within the wavelength regions $3500\text{--}6800\text{\AA}$, with exposure times between 420 and 1800 s. Detailed information on the objects and specific observations is given in Table 1.

In this research, the data reduction was performed using the *Image Reduction and Analysis*

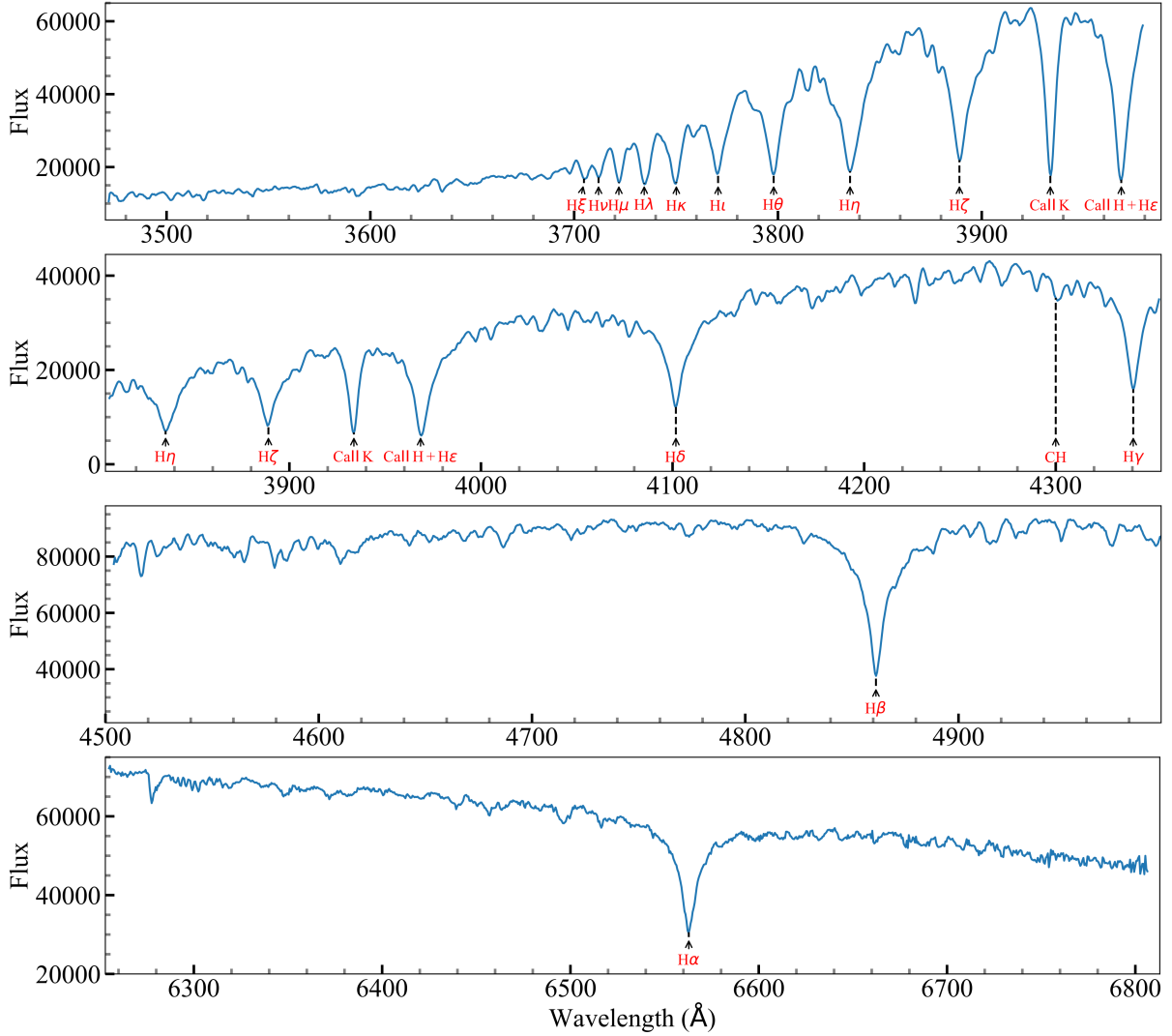


Figure 1: The wavelength-calibrated NUV and optical spectra of HR 8038, along with identified strong hydrogen and calcium lines, are shown as representative spectra.

Facility (`iraf`; Tody, 1986) software. In order to perform various operations, including initial bias, cosmic ray, and flat field corrections, identification of spectral lines, and wavelength calibrations, we used `iraf` packages, *viz.*, `imutil`, `crutil`, `noao.imred`, `noao.onedspec`, and `noao.twodspec`. For further operations with wavelength-calibrated spectra, we have also used Python packages, including `matplotlib` (Hunter, 2007), and `astropy` (Astropy Collaboration et al., 2022). A representative wavelength calibrated spectra of HR 8038, as observed on October 23, 2017, is shown in Fig. 1.

3. Spectral Fitting and Atmospheric Modeling

In order to investigate the photospheric absorption features, we initially computed steady-state 1-D plane-parallel model atmospheres in local thermodynamic equilibrium (LTE) with the ATLAS9 model (Kurucz, 1993; Castelli and Kurucz, 2003). To determine the stellar metallicity

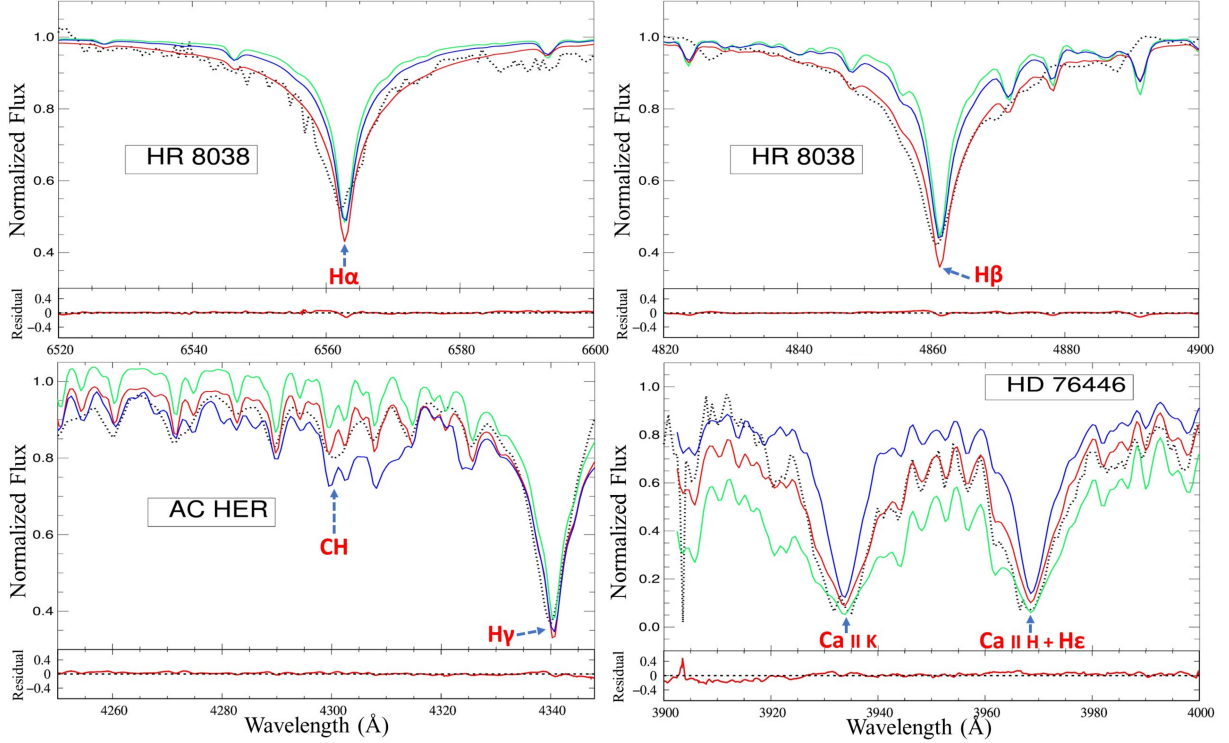


Figure 2: The spectral fitting of a few representative spectra is shown. The upper panel of each figure shows the observed spectra (black dotted line), best-fitted spectra (red solid line), and the typical variations from the best fit for a temperature and $\log g$ of 300 K and 1.0 dex (green and blue solid lines). The lower panel of each figure shows the residual of the observed and best-fitted spectra. In the top panel of each figure, the identified absorption lines have been marked with red-colored text and blue arrows, whereas the black label indicates the name of the corresponding low-mass star.

and detailed abundances, we used a realistic non-LTE version of the widely used state-of-the-art TURBOSPECTRUM synthesis code (Alvarez and Plez, 1998; Plez, 2012; Gerber et al., 2023).

We estimate the stellar parameters using the broad and strong H-features and Ca II H and K lines by iteratively varying the stellar parameters to arrive at the best fits. Fig. 2 shows a few representative absorption features of the program stars. The black dotted lines are the observed spectra, and the solid red lines show the best fit. The typical variations from the best-fit for a temperature variation of 300 K and $\log g$ variations of 1.0 dex are shown using green and blue solid lines, whereas the residuals of the observed and the best-fitted spectra are shown in the bottom panels. In the representative spectra shown in Fig. 2, we have marked the identified absorption features of H α , H β , Ca II H (along with He), Ca II K, H γ , and CH molecular band. The estimated best-fitted parameters of stellar surface temperature (T_{eff}), surface gravity ($\log g$), and metallicity ([Fe/H]) are given in Table 2. We also estimated the carbon abundance $A(C)$ from the absorption line at 4300 Å. The best-fitted carbon abundance is shown in the rightmost panel of Table 2.

Table 2: Estimated stellar parameters from the spectra. The solar carbon abundance $A(C)_{\odot}$ is adopted from (Grevesse et al., 2007), whereas the stellar abundance $A(C)_*$ is estimated as $A(C)_* = A(C) - A(C)_{\odot}$.

Object	T_{eff} (K)	$\log g$ (dex)	[Fe/H] (dex)	$A(C)_*$ (dex)
HR 8038	7100 ± 300	4.50 ± 0.5	-0.8 ± 0.3	-0.39 ± 0.50
AC Her	5650 ± 300	2.10 ± 0.5	-1.3 ± 0.3	-0.24 ± 0.45
HD 76446	5850 ± 300	4.00 ± 0.5	-0.5 ± 0.3	0.71 ± 0.40

4. Discussion and Conclusions

In this paper, we present an analysis of stellar parameters using low-resolution Near-UV and optical spectra. We estimated the surface temperatures of HR 8038, AC Her, and HD 76446 to be 7100, 5650, and 5850 K, respectively. In the literature, there are 17, 12, and 8 estimations of surface temperatures available for these three sources. The known surface temperatures of HR 8038, AC Her, and HD 76446 are found to be within the ranges of 7051–7850, 5080–5933, and 5730–6027 K, respectively. The surface gravities, on the other hand, are previously derived to be within the ranges of 3.69–3.99, 1.39–3.79, and 3.85–4.13, whereas the metallicities were estimated to be in the ranges of -1.08 to -0.46 , -1.35 to -0.75 , and -0.58 to $+0.03$, respectively. We found that seven out of nine parameters estimated from the spectral fitting are within the 1σ uncertainty level. Although the objects considered for this paper are well-studied, obtaining similar values for the stellar parameters using low-resolution spectra is an interesting finding. However, the only source HR 8038 shows a slight deviation in T_{eff} and a significant deviation in $\log g$, and it needs further investigation.

In order to estimate the carbon abundances, we used the best-fit values for T_{eff} , $\log g$, and [Fe/H]. The carbon abundances $A(C)$ of HR 8038, AC Her, and HD 76446 are estimated to be 8.0, 8.15, and 9.1. Considering the solar carbon abundance value of 8.39 (Grevesse et al., 2007), we found the carbon abundance of HR 8038, AC Her, and HD 76446 are 95%, 97%, and 108% of the solar value. We expect to report more results from the low-mass spectroscopic survey of MIRA with a robust investigation of spectral lines in the future. The analysis with the complete sample of 130 low-mass stars will provide useful information on stellar abundances and will further enable us to understand the First Ionization Potential effect on low-mass stars. This study will provide important information to understand the stellar magnetic dynamo and chemical evolution of the Galaxy.

Acknowledgments

This research is based on the observations obtained with the DPS instrument at MIRA/OOS. We acknowledge *Friends of MIRA* for supporting this research. This research uses ATLAS9 atmospheric model and TURBOSPECTRUM spectral synthesis code. This work is also supported by the Belgo-Indian Network for Astronomy and astrophysics (BINA), approved by the International

Division, Department of Science and Technology (DST, Govt. of India; DST/INT/BELG/P-09/2017) and the Belgian Federal Science Policy Office (BELSPO, Govt. of Belgium; BL/33/IN12).

Further Information

Authors' ORCID identifiers

0000-0001-8620-4511 (Subhajeet KARMAKAR)
0000-0002-8304-5444 (Avrajit BANDYOPADHYAY)
0009-0005-0584-3343 (William Bruce WEAVER)
0000-0002-2489-5908 (Riddhi SHEDGE)
0000-0002-4331-1867 (Jeewan Chandra PANDEY)
0000-0003-0340-7773 (Daniel Vincent COTTON)
0000-0002-6703-5406 (Jean PERKINS)

Author contributions

SK: Conceptualization, Project administration, Formal analysis (lead), Investigation (lead), Supervision (mentored intern RS), Software (IRAF, Python, SHELL), Visualization, Writing – Original Draft;

AB: Software (IDL, ATLAS9, TURBOSPECTRUM), Formal analysis (spectral fitting), Investigation (atmospheric modeling), Visualization, Writing – Review and Editing;

WBW: Investigation (observation), Writing – Review and Editing;

RS: Software (IRAF, SHELL), Formal analysis (data reduction), Investigation (wavelength calibration);

JCP: Investigation (stellar absorption features), Writing – Review and Editing;

DVC: Writing – Review and Editing;

JP: Writing – Review and Editing.

Conflicts of interest

The authors declare no conflict of interest.

References

- Alvarez, R. and Plez, B. (1998) Near-infrared narrow-band photometry of M-giant and Mira stars: models meet observations. *A&A*, 330, 1109–1119. <https://doi.org/10.48550/arXiv.astro-ph/9710157>.
- Astropy Collaboration, Price-Whelan, A. M., Lim, P. L., Earl, N., Starkman, N., Bradley, L., Shupe, D. L., Patil, A. A., Corrales, L., Brasseur, C. E., Nöthe, M., Donath, A., Tollerud,

E., Morris, B. M., Ginsburg, A., Vaher, E., Weaver, B. A., Tocknell, J., Jamieson, W., van Kerkwijk, M. H., Robitaille, T. P., Merry, B., Bachetti, M., Günther, H. M., Aldcroft, T. L., Alvarado-Montes, J. A., Archibald, A. M., Bódi, A., Bapat, S., Barentsen, G., Bazán, J., Biswas, M., Boquien, M., Burke, D. J., Cara, D., Cara, M., Conroy, K. E., Conseil, S., Craig, M. W., Cross, R. M., Cruz, K. L., D'Eugenio, F., Dencheva, N., Devillepoix, H. A. R., Dietrich, J. P., Eigenbrot, A. D., Erben, T., Ferreira, L., Foreman-Mackey, D., Fox, R., Freij, N., Garg, S., Geda, R., Glattly, L., Gondhalekar, Y., Gordon, K. D., Grant, D., Greenfield, P., Groener, A. M., Guest, S., Gurovich, S., Handberg, R., Hart, A., Hatfield-Dodds, Z., Homeier, D., Hosseinzadeh, G., Jenness, T., Jones, C. K., Joseph, P., Kalmbach, J. B., Karamehmetoglu, E., Kałuszyński, M., Kelley, M. S. P., Kern, N., Kerzendorf, W. E., Koch, E. W., Kulumani, S., Lee, A., Ly, C., Ma, Z., MacBride, C., Maljaars, J. M., Muna, D., Murphy, N. A., Norman, H., O'Steen, R., Oman, K. A., Pacifici, C., Pascual, S., Pascual-Granado, J., Patil, R. R., Perren, G. I., Pickering, T. E., Rastogi, T., Roulston, B. R., Ryan, D. F., Rykoff, E. S., Sabater, J., Sakurikar, P., Salgado, J., Sanghi, A., Saunders, N., Savchenko, V., Schwardt, L., Seifert-Eckert, M., Shih, A. Y., Jain, A. S., Shukla, G., Sick, J., Simpson, C., Singanamalla, S., Singer, L. P., Singhal, J., Sinha, M., Sipőcz, B. M., Spitler, L. R., Stansby, D., Streicher, O., Šumak, J., Swinbank, J. D., Taranu, D. S., Tewary, N., Tremblay, G. R., Val-Borro, M. d., Van Kooten, S. J., Vasović, Z., Verma, S., de Miranda Cardoso, J. V., Williams, P. K. G., Wilson, T. J., Winkel, B., Wood-Vasey, W. M., Xue, R., Yoachim, P., Zhang, C., Zonca, A. and Astropy Project Contributors (2022) The Astropy project: Sustaining and growing a community-oriented open-source project and the latest major release (v5.0) of the core package. *ApJ*, 935(2), 167. <https://doi.org/10.3847/1538-4357/ac7c74>.

Bailer-Jones, C. A. L., Rybizki, J., Fouesneau, M., Mantelet, G. and Andrae, R. (2018) Estimating distance from parallaxes. IV. Distances to 1.33 billion stars in *Gaia* Data Release 2. *AJ*, 156, 58. <https://doi.org/10.3847/1538-3881/aacb21>.

Bandyopadhyay, A., Sivarani, T., Beers, T. C., Susmitha, A., Nayak, P. K. and Pandey, J. C. (2022) Li distribution, kinematics, and detailed abundance analysis among very metal-poor stars in the Galactic halo from the HESP-GOMPA survey. *ApJ*, 937(2), 52. <https://doi.org/10.3847/1538-4357/ac8b0f>.

Beverage, A. G., Kriek, M., Conroy, C., Sandford, N. R., Bezanson, R., Franx, M., van der Wel, A. and Weisz, D. R. (2023) From carbon to cobalt: Chemical compositions and ages of $z \sim 0.7$ quiescent galaxies. *ApJ*, 948(2), 140. <https://doi.org/10.3847/1538-4357/acc176>.

Bochanski, J. J., Hawley, S. L., Covey, K. R., West, A. A., Reid, I. N., Golimowski, D. A. and Ivezić, Ž. (2010) The luminosity and mass functions of low-mass stars in the Galactic disk. II. The field. *AJ*, 139, 2679–2699. <https://doi.org/10.1088/0004-6256/139/6/2679>.

Bond, H. E., Nelan, E. P., VandenBerg, D. A., Schaefer, G. H. and Harmer, D. (2013) HD 140283: A star in the solar neighborhood that formed shortly after the big bang. *ApJ*, 765(1), L12. <https://doi.org/10.1088/2041-8205/765/1/L12>.

- Bond, J. C., O'Brien, D. P. and Lauretta, D. S. (2010) The compositional diversity of extrasolar terrestrial planets. I. In situ simulations. *ApJ*, 715(2), 1050–1070. <https://doi.org/10.1088/0004-637X/715/2/1050>.
- Botelho, R. B., Milone, A. d. C., Meléndez, J., Alves-Brito, A., Spina, L. and Bean, J. L. (2020) Carbon, isotopic ratio $^{12}\text{C}/^{13}\text{C}$, and nitrogen in solar twins: constraints for the chemical evolution of the local disc. *MNRAS*, 499(2), 2196–2213. <https://doi.org/10.1093/mnras/staa2917>.
- Carigi, L., Peimbert, M., Esteban, C. and García-Rojas, J. (2005) Carbon, nitrogen, and oxygen galactic gradients: A solution to the carbon enrichment problem. *ApJ*, 623(1), 213–224. <https://doi.org/10.1086/428491>.
- Castelli, F. and Kurucz, R. L. (2003) New grids of ATLAS9 model atmospheres. In *Modelling of Stellar Atmospheres*, edited by Piskunov, N., Weiss, W. W. and Gray, D. F., vol. 210. Astronomical Society of the Pacific. <https://doi.org/10.48550/arXiv.astro-ph/0405087>. Poster A20.
- Cescutti, G., Matteucci, F., McWilliam, A. and Chiappini, C. (2009) The evolution of carbon and oxygen in the bulge and disk of the Milky Way. *A&A*, 505(2), 605–612. <https://doi.org/10.1051/0004-6361/200912759>.
- Chiappini, C., Matteucci, F. and Meynet, G. (2003) Stellar yields with rotation and their effect on chemical evolution models. *A&A*, 410, 257–267. <https://doi.org/10.1051/0004-6361:20031192>.
- Gerber, J. M., Magg, E., Plez, B., Bergemann, M., Heiter, U., Olander, T. and Hoppe, R. (2023) Non-LTE radiative transfer with Turbospectrum. *A&A*, 669, A43. <https://doi.org/10.1051/0004-6361/202243673>.
- Grant, D., Lothringer, J. D., Wakeford, H. R., Alam, M. K., Alderson, L., Bean, J. L., Benneke, B., Désert, J.-M., Daylan, T., Flagg, L., Hu, R., Inglis, J., Kirk, J., Kreidberg, L., López-Morales, M., Mancini, L., Mikal-Evans, T., Molaverdikhani, K., Palle, E., Rackham, B. V., Redfield, S., Stevenson, K. B., Valenti, J. A., Wallack, N. L., Aggarwal, K., Ahrer, E.-M., Crossfield, I. J. M., Crouzet, N., Iro, N., Nikolov, N. K., Wheatley, P. J. and JWST Transiting Exoplanet Community ERS Team (2023) Detection of carbon monoxide's 4.6 micron fundamental band structure in WASP-39b's atmosphere with JWST NIRSpec G395H. *ApJ*, 949(1), L15. <https://doi.org/10.3847/2041-8213/acd544>.
- Grevesse, N., Asplund, M. and Sauval, A. J. (2007) The solar chemical composition. *SSRv*, 130(1-4), 105–114. <https://doi.org/10.1007/s11214-007-9173-7>.
- Gustafsson, B. (2022) Chemical tracing and the origin of carbon in the Galactic disk. *Univ*, 8(8), 409. <https://doi.org/10.3390/universe8080409>.
- Hunter, J. D. (2007) Matplotlib: A 2D graphics environment. *CSE*, 9(3), 90–95. <https://doi.org/10.1109/MCSE.2007.55>.

Hutter, D. J., Elias, I., N. M., Peterson, E. R., Weaver, W. B., Weaver, G., Mozurkewich, D., Vrba, F. J., Simon, R. S., Buscher, D. F. and Hummel, C. A. (1997) Seeing tests at four sites in support of the NPOI project. *AJ*, 114, 2822–2933. <https://doi.org/10.1086/118690>.

Jofré, P., Heiter, U., Soubiran, C., Blanco-Cuaresma, S., Worley, C. C., Pancino, E., Cantat-Gaudin, T., Magrini, L., Bergemann, M., González Hernández, J. I., Hill, V., Lardo, C., de Laverny, P., Lind, K., Masseron, T., Montes, D., Mucciarelli, A., Nordlander, T., Recio Blanco, A., Sobeck, J., Sordo, R., Sousa, S. G., Tabernero, H., Vallenari, A. and Van Eck, S. (2014) *Gaia* FGK benchmark stars: Metallicity. *A&A*, 564, A133. <https://doi.org/10.1051/0004-6361/201322440>.

Karmakar, S. (2019) Evolution of magnetic activities in Late-type stars. Ph.D. thesis, ARIES, Nainital, India; PRSU, Raipur, India. <https://doi.org/10.5281/zenodo.5762548>.

Karmakar, S., Naik, S., Pandey, J. C. and Savanov, I. S. (2022) *AstroSat* observations of long-duration X-ray superflares on active M-dwarf binary EQ Peg. *MNRAS*, 509(3), 3247–3257. <https://doi.org/10.1093/mnras/stab3099>.

Karmakar, S., Naik, S., Pandey, J. C. and Savanov, I. S. (2023) *Swift* and *XMM–Newton* observations of an RS CVn-type eclipsing binary SZ Psc: superflare and coronal properties. *MNRAS*, 518(1), 900–918. <https://doi.org/10.1093/mnras/stac2970>.

Karmakar, S., Pandey, J. C., Airapetian, V. S. and Misra, K. (2017) X-ray superflares on CC Eri. *ApJ*, 840(2), 102. <https://doi.org/10.3847/1538-4357/aa6cb0>.

Karmakar, S., Pandey, J. C., Naik, S., Savanov, I. S. and Raj, A. (2019) Magnetic activities on active solar-type stars. *BSRSL*, 88, 182–189. <https://doi.org/10.48550/arXiv.1905.13512>.

Karmakar, S., Pandey, J. C., Savanov, I. S., Taş, G., Pandey, S. B., Misra, K., Joshi, S., Dmitrienko, E. S., Sakamoto, T., Gehrels, N. and Okajima, T. (2016) LO Peg: surface differential rotation, flares, and spot-topographic evolution. *MNRAS*, 459(3), 3112–3129. <https://doi.org/10.1093/mnras/stw855>.

Kurucz, R. L. (1993) Atomic data for interpreting stellar spectra: isotopic and hyperfine data. *PhST*, 47, 110–117. <https://doi.org/10.1088/0031-8949/1993/T47/017>.

Madhusudhan, N., Lee, K. K. M. and Mousis, O. (2012) A possible carbon-rich interior in super-Earth 55 Cancri e. *ApJ*, 759(2), L40. <https://doi.org/10.1088/2041-8205/759/2/L40>.

Pelletier, S., Benneke, B., Darveau-Bernier, A., Boucher, A., Cook, N. J., Piaulet, C., Coulombe, L.-P., Artigau, É., Lafrenière, D., Delisle, S., Allart, R., Doyon, R., Donati, J.-F., Fouqué, P., Moutou, C., Cadieux, C., Delfosse, X., Hébrard, G., Martins, J. H. C., Martioli, E. and Vandal, T. (2021) Where is the water? Jupiter-like C/H ratio but strong H₂O depletion found on τ boötis b using SPIRou. *AJ*, 162(2), 73. <https://doi.org/10.3847/1538-3881/ac0428>.

Plez, B. (2012) Turbospectrum: Code for spectral synthesis. Astrophysics Source Code Library, record ascl:1205.004.

Priest, E. (2000) Sun and solar-terrestrial physics. In Encyclopedia of Astronomy & Astrophysics, edited by Murdin, P. Institute of Physics Publishing, Bristol (UK). <https://doi.org/10.1888/0333750888/5397>.

Romano, D., Franchini, M., Grisoni, V., Spitoni, E., Matteucci, F. and Morossi, C. (2020) The variation of carbon abundance in galaxies and its implications. *A&A*, 639, A37. <https://doi.org/10.1051/0004-6361/202037972>.

Tody, D. (1986) The Iraf data reduction and analysis system. In Instrumentation in Astronomy VI, edited by Crawford, D. L., vol. 0627, pp. 733 – 748. International Society for Optics and Photonics, SPIE. <https://doi.org/10.1117/12.968154>.

Torres-Dodgen, A. V. and Weaver, W. B. (1993) An atlas of low-resolution near-infrared spectra of normal stars. *PASP*, 105, 693. <https://doi.org/10.1086/133222>.

Walker, M. F. (1970) The California Site Survey. *PASP*, 82(487), 672. <https://doi.org/10.1086/128945>.

Walker, R. G., Weaver, W. B., Shane, W. W. and Babcock, A. (2007) Deep impact: Optical spectroscopy and photometry obtained at MIRA. *Icar*, 191(2), 526–536. <https://doi.org/10.1016/j.icarus.2006.10.046>.

Weaver, W. B. (1975) Monterey Institute for Research in Astronomy, Carmel Valley, California. Observatory report. *BAAS*, 7, 152–153.

Zhang, X., Buder, S., Wu, Y.-Q. and Zhao, G. (2021) Estimation of ages and masses via carbon and nitrogen abundances for 556 007 giants from LAMOST. *RAA*, 21(9), 216. <https://doi.org/10.1088/1674-4527/21/9/216>.